

# Normal-Relaxor-Diffuse Ferroelectric Phase Transition and Electrical Properties of $\text{Bi}(\text{Mg}_{1/2}\text{Ti}_{1/2})_3\text{-PbZrO}_3\text{-PbTiO}_3$ Solid Solution Ceramics Near the Morphotropic Phase Boundary

Haifeng Yi and Ruzhong Zuo<sup>†</sup>

Institute of Electro Ceramics &amp; Devices, School of Materials Science and Engineering, Hefei University of Technology, Hefei 230009, China

**Perovskite-type  $x\text{Bi}(\text{Mg}_{1/2}\text{Ti}_{1/2})_3\text{O}_3\text{-(0.56 - }x)\text{PbZrO}_3\text{-0.44 PbTiO}_3$  ( $x\text{BMT-PZ-PT}$ ) ternary solid solution ceramics were synthesized via a conventional solid-state reaction method. The phase transition behaviors, dielectric, ferroelectric, and piezoelectric properties were investigated as a function of the BMT content. The X-ray diffraction analysis showed that the tetragonality of  $x\text{BMT-PZ-PT}$  was enhanced with increasing the BMT content, and a morphotropic phase boundary (MPB) between rhombohedral and tetragonal phases was identified approximately in the composition of  $x = 0.08$ . In addition, the dielectric diffuseness and frequency dispersion behavior were induced with the addition of BMT and a normal-relaxor-diffuse ferroelectric transformation was observed from the PZ-rich side to the BMT-rich side. The electrical properties of  $x\text{BMT-PZ-PT}$  ceramics exhibit obviously compositional dependence. The  $x = 0.08$  composition not only possessed the optimum properties with  $\epsilon'_{33}/\epsilon_0 = 1450$ ,  $Q_m = 69$ ,  $d_{33} = 390$  pC/N,  $k_p = 0.46$ ,  $P_r = 30$   $\mu\text{C}/\text{cm}^2$ ,  $E_c = 1.4$  kV/mm,  $T_c = 325^\circ\text{C}$ , and a strain of 0.174% ( $d_{33}^* = 436$  pm/V) under an electric field of 4 kV/mm as a result of the coexistence of two ferroelectric phases near the MPB, but also owned a good thermal-depolarization behavior with a  $d_{33}$  value of  $>315$  pC/N up to  $290^\circ\text{C}$  and a frequency-insensitive strain behavior.**

## I. Introduction

LEAD-BASED perovskite structured binary piezoelectric ceramics, such as  $\text{PbZrO}_3\text{-PbTiO}_3$  (PZT), have been widely investigated and used for actuators and sensors due to their excellent piezoelectric performances.<sup>1,2</sup> The high piezoelectric activity should be achieved near a morphotropic phase boundary (MPB) where two adjacent phases with different lattice distortions in a phase diagram have equal Gibbs free energies.<sup>3–5</sup> On the other hand, forming a ternary solid solution between PZT and some lead-based relaxor ferroelectrics is an important route to further improve their electrical properties, such as  $\text{Pb}(\text{Me}_{1/3}\text{Nb}_{2/3})\text{O}_3$ -type (Me:  $\text{Mg}^{2+}$ ,  $\text{Zn}^{2+}$ ,  $\text{Ni}^{2+}$ , etc.) complex perovskites, because these relaxor ferroelectrics might have better dielectric properties.<sup>6–8</sup> Recently, however, the application of lead-based ceramics has been challenged for their relatively low Curie points ( $T_c$ ) and brought about serious lead pollution due to their high toxicity. Thus, the lead-free and low-lead content piezoelectric ceramics have attracted much attention. Unfortunately, the currently focused lead-free ferroelectric systems such as titanate- or niobate-based compositions have exhibited either

processing difficulties or stability issues of piezoelectric properties,<sup>9</sup> which could make them quite hard to be applied in industry. In contrast, it should be meaningful and applicable to develop lead-reduced piezoelectric ceramics to satisfy the requirements of industry.

Nowdays, bismuth-based compositions are widely considered as nontoxic substitutes for lead-based compositions. Indeed,  $\text{Bi}^{3+}$  and  $\text{Pb}^{2+}$  possess the same lone-pair electronic configurations and majority of the Bi-containing oxygen octahedral compounds are known to demonstrate good ferroelectric properties.<sup>10</sup> Bi-based perovskites compounds such as  $\text{BiMeO}_3$ , in which Me are cations with a valence of +3 (Me:  $\text{Fe}^{3+}$ ,  $\text{Sc}^{3+}$ ,  $\text{Ni}_{1/2}\text{Ti}_{1/2}$ ,  $\text{Mg}_{1/2}\text{Ti}_{1/2}$ , and  $\text{Zn}_{1/2}\text{Ti}_{1/2}$ , etc.) are typical lead-free ferroelectrics and have been largely investigated in recent years.<sup>11–15</sup> Among the  $\text{BiMeO}_3$  members,  $\text{Bi}(\text{Mg}_{1/2}\text{Ti}_{1/2})_3$  (BMT) shows a structure of rhombohedral symmetry at room temperature and needs to be synthesized under high-pressure and high-temperature conditions.<sup>16</sup> Recently, it has been shown that BMT can be stabilized in the solid solutions with other perovskite end members. For instance,  $(1 - x)\text{BMT-}x\text{PT}$  is one of the most promising candidates for high-temperature applications due to its high  $T_c$  ( $478^\circ\text{C}$ ,  $x = 0.37$ ), reasonable piezoelectric properties (e.g.,  $d_{33} = 225$  pC/N,  $k_p = 0.38$ ) and low cost.<sup>17–20</sup> Nevertheless, there are still a few disadvantages in this system such as relatively high conductivity and high coercive fields, which make it hard to be well poled. So if we combine BMT-PT with PZT, it is reasonable to believe that excellent electrical properties can be achieved near the MPB region of a new ternary solid solution system of BMT-PZ-PT. Although this ternary system was studied by Chen *et al.*<sup>21</sup> and Fu *et al.*<sup>22</sup> in terms of its electrostrains under a high external electric field, yet, a full study on their phase transformation behavior and compositional dependence of dielectric, ferroelectric, and piezoelectric properties has been still missing.

In this work, a new MPB composition system of  $x\text{Bi}(\text{Mg}_{1/2}\text{Ti}_{1/2})_3\text{O}_3\text{-(0.56 - }x)\text{PbZrO}_3\text{-0.44PbTiO}_3$  ( $x\text{BMT-PZ-PT}$ ) was constructed by substituting BMT for PZ at a fixed content of PT. The purpose of this study was then to identify how the phase structure of  $x\text{BMT-PZ-PT}$  changes with the BMT content and simultaneously to explore the composition dependence of electrical properties. The thermal stability and frequency dependence of piezoelectric and electromechanical properties were investigated as well.

## II. Experimental Procedures

The  $x\text{BMT-(0.56 - }x)\text{PZ-0.44PT}$  ( $x\text{BMT-PZ-PT}$ ,  $x = 0\text{--}0.56$ ) ceramics were synthesized by a conventional solid-state reaction method using high-purity oxides:  $\text{Bi}_2\text{O}_3$  ( $\geq 99.0\%$ ),  $\text{PbO}$  ( $\geq 99.0\%$ ),  $\text{ZrO}_2$  ( $\geq 99.0\%$ ),  $\text{TiO}_2$  ( $\geq 99.0\%$ ), and  $(\text{MgCO}_3)_4\cdot\text{Mg}(\text{OH})_2\cdot 5\text{H}_2\text{O}$  ( $\geq 99.0\%$ ) as raw materials. The powders were weighted and ball-milled with ethanol and zirconia media for

J. C. Nino—contributing editor

4 h, then the slurry was dried at 100°C and calcined twice in a closed alumina crucible at 850°C for 2 h. After calcination, the mixture was ball-milled again for 6 h with 0.5 wt% PVB as a binder. The granulated powder was uniaxially pressed into disks with a diameter of 10 mm and a thickness of 1 mm. The compacted disks were sintered in the temperature range 1050°C–1200°C for 2 h. To minimize the vaporization of Bi and Pb, sample disks were buried in the sacrificial powder of the same composition. For the electrical measurements, silver paste was painted on major sides of the disks and then fired at 650°C for 30 min as the electrodes. The specimens were polarized in a silicone oil bath at 100°C under a dc field of 3–4 kV/mm for 15 min.

The phase structures were analyzed at room temperature by the X-ray diffractometer (XRD, D/Mzx-rB; Rigaku, Tokyo, Japan) with  $\text{CuK}\alpha_1$  radiation. The dielectric properties were measured at various frequencies using an LCR meter (Agilent E4980A, Santa Clara, CA) in a temperature range 25°C–550°C and at a frequency range 0.1 kHz–1 MHz. The piezoelectric strain constant  $d_{33}$  of poled samples was measured by a Belincourt-meter (YE2703A; Sinocera, Yangzhou, China). The planar electromechanical coupling factor  $k_p$  and the mechanical quality factor  $Q_m$  were determined by a resonance–antiresonance method with an impedance analyzer (PV70A; Beijing Band ERA Co. Ltd., Beijing, China). A ferroelectric test system (Precision LC, Radiant Technologies, Inc. Albuquerque, NM) was used to measure the polarization–electric field ( $P$ – $E$ ) hysteresis loops and electric-field-induced strain ( $S$ – $E$ ) curves. Thermal depoling experiments were conducted by annealing the poled samples at various temperatures for 15 min 24 h after poling, cooling to room temperature, and then measuring their  $d_{33}$  and  $k_p$  values.

### III. Results and Discussion

Figure 1 shows a schematic phase diagram of the BMT–PZ–PT ternary system based on the work of Jaffe *et al.*<sup>1</sup> and Randall *et al.*<sup>17</sup> in which the blue dashed line stands for the approximate position of the MPB for the BMT–PZ–PT ternary system. The selected compositions were plotted as red dots and located on both sides of the MPB by fixing a PT content of 44%. It is thus expected that the substitution of BMT for PZ was found to induce a morphotropic phase structural transformation from rhombohedral to tetragonal ferroelectric phases. Figure 2 illustrates the room-temperature XRD patterns of  $x$ BMT–PZ–PT ceramics. As can be seen, all compositions demonstrate a pure perovskite structure without any deleterious phases in terms of typical diffraction patterns as shown in Fig. 2(a). This indicates that  $\text{Bi}^{3+}$  and  $(\text{Mg}_{1/2}^{2+}\text{Ti}_{1/2}^{4+})$  can diffuse completely into the PZT matrix lattice to form a homogeneous solid solution. Moreover, a phase transition from rhombohedral to tetragonal with an increase in the BMT content was detected. The difference between these two phase structures can be characterized by the (200)-diffraction peaks around 45°. Figure 2(b) presents the (200)-diffraction peaks at 43°–47°. It is observed that there was no observable peak splitting for the compositions with  $x \leq 0.06$ , indicating that these compositions have a pure rhombohedral symmetry. When  $x \geq 0.1$ , the (200) peak tends to split and the splitting becomes more and more obvious, generally suggesting that a tetragonal structure appears and becomes stronger. Figure 2(c) shows the (200) diffraction peaks of the  $x = 0.04, 0.08, \text{ and } 0.14$  compositions. The fitting analysis of the diffraction peak profiles was carried out by using pseudo-Voigt peak shape function. The symmetry of the samples can be well established from the peak splitting and the relative intensity of these reflection lines. It can be clearly seen that a transition from a rhombohedral phase for the  $x = 0.04$  samples to a tetragonal phase for the  $x = 0.14$  sample. The  $(002)_T/(200)_T$  and  $(200)_R$  peaks could be simultaneously detected in the  $x = 0.08$  sample.

From the above results, it is clear that the phase structure of  $x$ BMT–PZ–PT ceramics changes from the rhombohedral structure to the tetragonal structure with increasing the BMT content. The  $x = 0.08$  sample should be an MPB composition with a coexistence of both rhombohedral and tetragonal phases.

Figure 3 shows the temperature and frequency dependencies of the dielectric permittivity and loss tangent of the unpoled  $x$ BMT–PZ–PT ceramics. From Figs. 3(a)–(g), it can be obviously seen that the dielectric behavior of the  $x$ BMT–PZ–PT ceramics changes drastically with the addition of BMT. The PZ–PT ( $x = 0$ ) binary composition exhibits an evident normal ferroelectric phase transition behavior. With increasing the BMT content, the ternary solid solution exhibits more relaxor-like characteristics, showing that the dielectric peaks at the dielectric maxima become more diffuse and more frequency-dependent. The diffuseness of the phase transition can be described by the modified Curie-Weiss law,<sup>23</sup> which can be expressed as  $1/\varepsilon - 1/\varepsilon_m = C^{-1}(T - T_m)^\gamma$  where  $\varepsilon_m$  is the maximum value of the dielectric permittivity at the transition temperature  $T_m$ ,  $C$  is the Curie-like constant, and  $\gamma$  is the degree of diffuseness which varies between 1 for a normal ferroelectric and 2 for an ideal relaxor ferroelectric. The  $\gamma$  value of different compositions can be determined from the slopes of linearly fitted lines as shown in Fig. 3(h). It can be seen that the  $\gamma$  value of the  $x$ BMT–PZ–PT ternary solid solution increases with increasing the BMT content as  $x < 0.56$ , which indicates that the relaxor characteristics becomes more distinct. There are two mechanisms for the observed relaxor behavior. One is attributed to the inhomogeneous distribution of B-site cations in an  $\text{ABO}_3$  perovskite structure and another is attributed to the defect relaxation related to oxygen vacancies.<sup>24</sup> When  $x = 0.56$ , the BMT–PT binary composition owns  $\gamma = 1.77$  but  $\Delta T_{\text{relax}} = 0$ , which is defined as the difference between  $T_m$  values measured at 1 kHz and 1 MHz,<sup>25</sup> indicating that this composition owns a typical diffuse phase transition behavior with no frequency dispersion. This is usually considered as an intermediate state between normal ferroelectrics and relaxor ferroelectrics.<sup>26</sup> The above change means that there is a normal-relaxor-diffuse ferroelectric transformation in the studied compositions from the PZ-rich side to the BMT-rich side. In addition, the corresponding loss tangent was found to decrease with increasing the BMT content unless the pure BMT–PT. A relatively high loss tangent was also previously reported for pure BMT–PT sample.<sup>17,22</sup> Nevertheless, the loss value can retain less than 0.07 in the temperature range from room temperature to ~250°C at a frequency of over 1 kHz, suggesting a potential for high-temperature applications. However, the loss value significantly increases at higher temperatures, which is possibly attributed to the formation

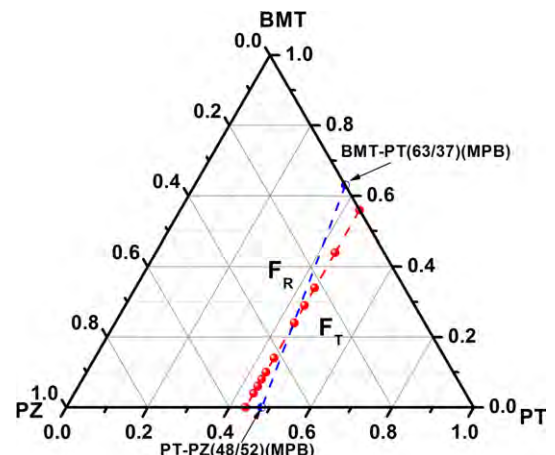


Fig. 1. Schematic phase diagram of BMT–PZ–PT ternary system.



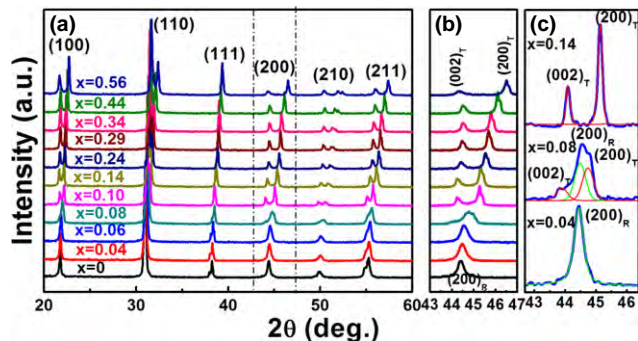


Fig. 2. (a) Room-temperature XRD full patterns of  $x$ BMT-PZ-PT ceramics, (b) Locally enlarged diffraction peaks in the  $2\theta$  range  $43^\circ$ – $47^\circ$ , and (c) Peak fitting analysis for the compositions with  $x = 0.04$ ,  $0.08$ , and  $0.14$ .

of thermally activated space charges. This conduction feature has been also reported in  $\text{BiScO}_3$ -PT ceramics.<sup>27</sup> The volatilization of Bi and Pb during sintering might be one of reasons for highly conductive characteristics of  $x$ BMT-PZ-PT ceramics. This drawback would degrade the piezoelectric and electromechanical properties of this system to a certain degree considering the difficulty in electrical poling.

Figure 4(a) presents the dielectric permittivity  $\epsilon_r$  at a fixed frequency of 10 kHz as a function of temperature for some typical unpoled  $x$ BMT-PZ-PT ceramics. For pure PZ-PT, a narrow peak was found for a normal ferroelectric ceramic. As the amount of BMT ( $x$ ) was increased, the dielectric peak was found to become broader and broader, indicating a typical relaxor ferroelectric behavior as discussed above in Fig. 3. This is possibly as a result of the increase in random fields caused by the enhanced cation disorder degree at both A-sites and B-sites ions.<sup>28</sup> Moreover, it can be seen from Fig. 4(b) that the dielectric maxima  $\epsilon_m$  reaches a maximum value at  $x = 0.08$ , indicating that the phase coexisted composition usually exhibits an enhanced dielectric property. In comparison, the variation in  $T_m$  does not show particular trend with increasing the BMT content. It first decreases from  $358^\circ\text{C}$  for  $x = 0$  sample up to  $285^\circ\text{C}$  for the  $x = 0.24$  sample, and then starts to increase afterwards. Generally, the

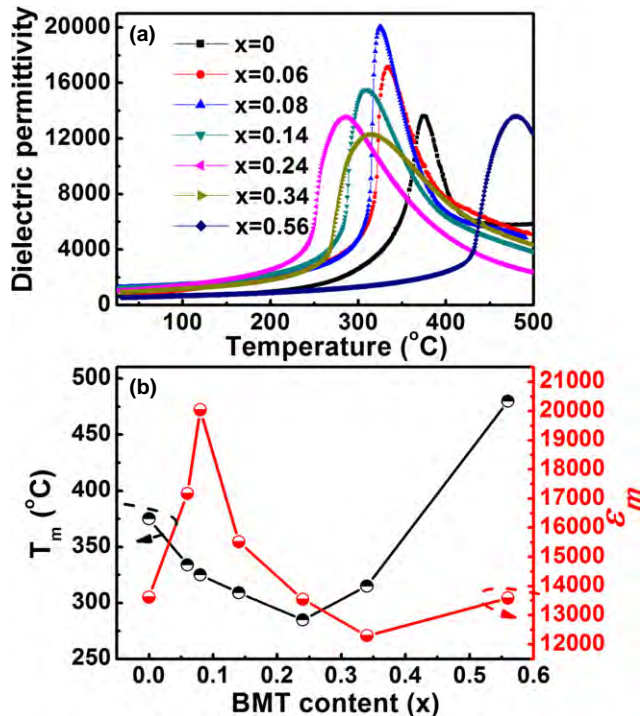


Fig. 4. (a) Dielectric permittivity versus temperature curves measured at 10 kHz for  $x$ BMT-PZ-PT ceramics as indicated, (b) The corresponding  $T_m$  and  $\epsilon_m$  values as a function of the BMT content.

decline in  $T_m$  corresponds to a decrease in tetragonality for a couple of perovskite solid solution ceramics, such as PZT and  $\text{BiMeO}_3$ -PT systems. It seems that the addition of BMT tends to enhance the tetragonality [see Fig. 2(a)], which should be responsible for the increase in  $T_m$  as  $x \geq 0.24$ . As  $x < 0.24$ , the variation in  $T_m$  in this study cannot be well explained in the same way. There are probably two competitive causes responsible for the change in the  $T_m$  value in the studied ternary system. The rhombohedral to tetragonal ferroelectric phase transition was usually accompanied by a rise of the  $T_m$  value as observed in a fewer perovskite-structured

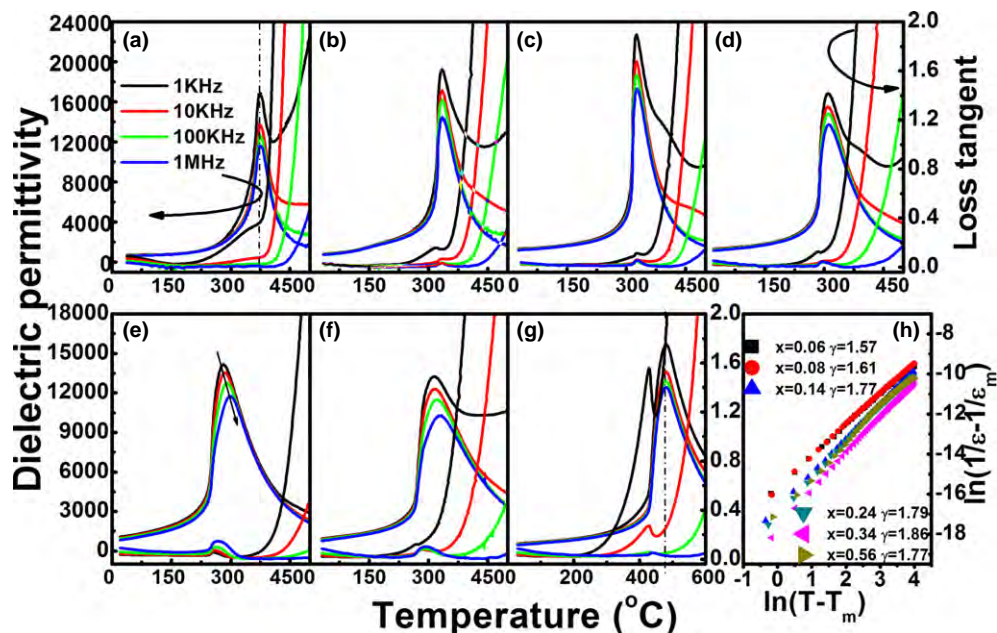


Fig. 3. Dielectric permittivity and loss tangent for selected  $x$ BMT-PZ-PT ceramics as a function of temperature and frequency: (a)  $x = 0$ , (b)  $x = 0.06$ , (c)  $x = 0.08$ , (d)  $x = 0.14$ , (e)  $x = 0.24$ , (f)  $x = 0.34$ , (g)  $x = 0.56$ , and (h) a plot of  $\ln(1/\epsilon - 1/\epsilon_m)$  as a function of  $\ln(T - T_m)$  at 10 kHz for selected samples.

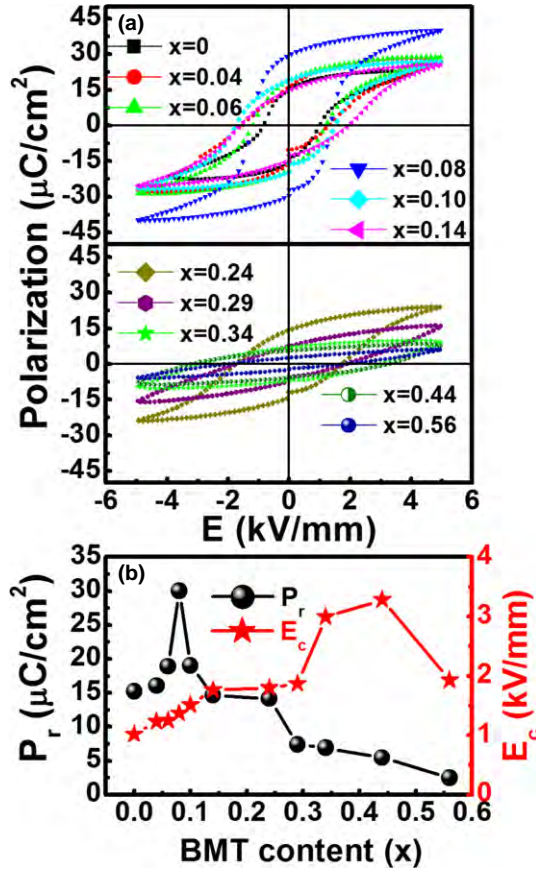


Fig. 5. (a)  $P$ - $E$  hysteresis loops of the  $x$ BMT-PZ-PT ceramics, (b) The values of  $P_r$  and  $E_c$  as a function of the BMT content.

piezoelectric ceramics, basically because of the enhanced tetragonality. Moreover, the observed composition-induced normal to relaxor phase transition usually tends to reduce the  $T_m$  values because of the weakening of the ferroelectric order degree.<sup>29</sup> The first reason might be dominant for the  $x > 0.24$  samples, and the second reason might mainly contribute to the  $x < 0.24$  compositions.

The ferroelectricity of  $x$ BMT-PZ-PT ceramics was characterized by measuring  $P$ - $E$  hysteresis loops at 1 Hz at room temperature, as shown in Fig. 5(a). The remanent polarization ( $P_r$ ) and the coercive fields ( $E_c$ ) values as a function of BMT content ( $x$ ) are given in Fig. 5(b). It can be observed from the shape of the hysteresis loops that all samples are of typical ferroelectrics and changes markedly with the addition of BMT. The  $x = 0$  sample (0.56PZ-0.44PT) prepared in this study showed similar both ferroelectric and piezoelectric properties to those reported previously for similar compositions.<sup>30,31</sup> The  $P_r$  value was found to firstly increase and reach a maximum value of  $30 \mu\text{C}/\text{cm}^2$  at  $x = 0.08$ , and then decrease rapidly upon increasing  $x$ . Due to the coexistence of ferroelectric rhombohedral and tetragonal phases in the

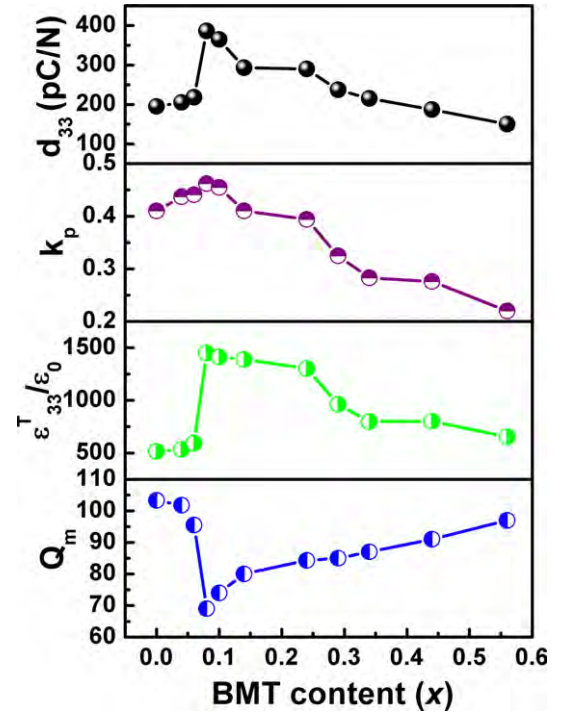


Fig. 6. Dielectric and piezoelectric properties of poled  $x$ BMT-PZ-PT ceramics sintered at optimum temperatures as a function of the BMT content.

MPB region, The highest  $P_r$  value can be expected due to the summation of the possible crystallographic orientations, eight  $\langle 111 \rangle$  spontaneous polarization directions in a rhombohedral phase and six  $\langle 001 \rangle$  directions in a tetragonal phase, which make the domain switching easier.<sup>32</sup> Meanwhile,  $E_c$  was found to increase from 1.02 to 3.28 kV/mm from the  $x = 0$  sample to the  $x = 0.44$  sample, which should be generally attributed to the enhanced tetragonality based on the fact that the domain walls are partially clamped in tetragonal phases by larger local internal stresses from the structural distortion in the polarization process (large  $c/a$  ratio). A relatively low  $E_c$  value was observed for the  $x = 0.56$  sample probably because this composition usually has a high leakage current in addition to its high tetragonality,<sup>18</sup> such that the  $P$ - $E$  loop was poorly saturated.

Figure 6 shows the dielectric and piezoelectric properties for poled  $x$ BMT-PZ-PT solid solution ceramics sintered at their optimum temperatures. It can be seen that the dielectric and piezoelectric properties exhibit obviously compositional dependences. With increasing the BMT content, they first dramatically increase with  $x$ , and reach the maxima at  $x = 0.08$ , after that start to decline. Therefore it can be confident that the MPB plays a crucial role in improving piezoelectric properties. The reason may be that the multiple polarization states can be more susceptibly switched along the direction of the external electric field, making the

Table I. Dielectric and Piezoelectric Properties of BiMeO<sub>3</sub>-PZ-PT Ternary Solid Solution Ceramics

Compounds	MPB ( $x$ )	$T_c$ ( $^{\circ}\text{C}$ )	$k_p$	$d_{33}$ (pC/N)	$\epsilon_{33}^T/\epsilon_0$	Ref.
$(0.9 - x)\text{BMT}-x\text{PT}-0.1\text{PZ}$	0.4	$\sim 450$	—	260	—	[21]
$x\text{BZT}-(1 - x)\text{PZ}_{0.56}\text{T}_{0.44}$	0.18	$\sim 260$	—	365	1430	[28]
$x\text{BZT}-(1 - x)\text{PZ}_{0.52}\text{T}_{0.48}$	0.15	—	0.45	319	1325	[33]
$x(0.3\text{BZT}-0.7\text{PT})-(1 - x)\text{PZ}$	0.52	$\sim 291$	—	311	1080	[34]
$0.1\text{BZT}-0.9[x\text{PT}-(1 - x)\text{PZ}]$	0.445	$\sim 320$	0.45	300	978	[35]
$x\text{BNT}-(0.9 - x)\text{PT}-0.1\text{PZ}$	0.47	$\sim 295$	—	317	1100	[36]
$0.511\text{BFO}-0.326\text{PZ}-0.163\text{PT}$	—	$\sim 431$	0.5	101	371	[37]
$x\text{BMT}-(0.56 - x)\text{PZ}-0.44\text{PT}$	0.08	$\sim 325$	0.46	390	1450	This study



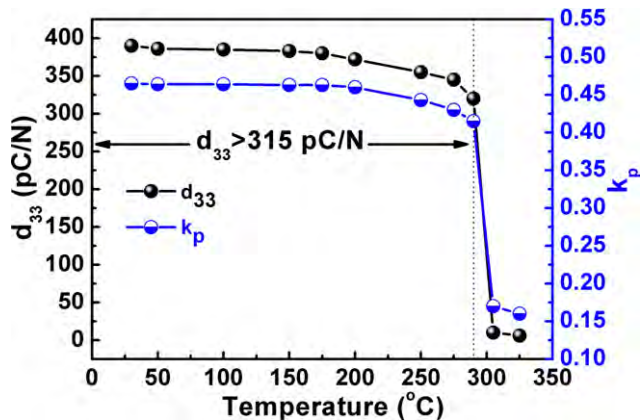


Fig. 7. The thermal stability of  $d_{33}$  and  $k_p$  values for the poled  $x = 0.08$  sample.

materials more electrically active, and thereby enhancing the piezoelectric response. By comparison,  $Q_m$  shows an opposite tendency with increasing  $x$ . The best dielectric and piezoelectric properties of  $\epsilon_{33}^T/\epsilon_0 = 1450$ ,  $Q_m = 69$ ,  $d_{33} = 390$  pC/N, and  $k_p = 0.46$  appear in the composition with  $x = 0.08$ , which are superior to those of pure Pb ( $Zr_{0.52}Ti_{0.48}$ ) $O_3$ <sup>1</sup> and 0.63BMT–0.37PT.<sup>17</sup> The comparison of the electrical properties between BiMeO<sub>3</sub>–PZ–PT systems such as BZT–PZ–PT<sup>27,33–35</sup> and Bi(Ni<sub>1/2</sub>Ti<sub>1/2</sub>)O<sub>3</sub> (BNT)–PZ–PT<sup>36</sup> was made in Table I. Although BiFeO<sub>3</sub> (BFO)–PZ–PT<sup>37</sup> system was reported to have a much higher  $T_c$  value, yet, its dielectric and piezoelectric properties are relatively low. It can be seen that the BMT–PZ–PT system possesses relatively high  $T_c$  and high piezoelectric properties. Figure 7 reveals the thermal stability of  $d_{33}$  and  $k_p$  values for the  $x = 0.08$  sample. The sample is open-circuited during annealing, but short-circuited before  $d_{33}$  and  $k_p$  values are remeasured at each chosen temperature ( $T_a$ ). This is an easy and convenient method for evaluating the thermal stability of piezoelectric properties. It should be also good enough to compare the property response since the samples in the current method may experience more heating cycles than in the in-situ measurement. It can be seen that the  $d_{33}$  and  $k_p$  values decrease only slightly with increasing depoling temperature ( $T_a \leq 290^\circ\text{C}$ ), and begin to sharply drop with further increasing  $T_a$  ( $T_a > 290^\circ\text{C}$ ) due to the fact that  $T_a$  is approaching the  $T_c$  ( $325^\circ\text{C}$ ). Nevertheless, a high  $d_{33}$  value ( $>315$  pC/N) can be maintained in the  $T_a$  range  $30^\circ\text{C}$ – $290^\circ\text{C}$ , demonstrating a good thermal stability of piezoelectric properties for the studied composition.

Figure 8 presents the unipolar electric-field-induced strain curves of  $x$ BMT–PZ–PT ceramics, measured under a relatively low electric field of 4 kV/mm at room temperature. The normalized strain  $d_{33}^*$ , which was defined as  $S_{\max}/E_{\max}$  where  $S_{\max}$  is the strain value at the maximum electric field ( $E_{\max}$ ), was summarized in the inset of Fig. 8. An obviously composition-dependent strain behavior was observed in  $x$ BMT–PZ–PT ceramics with varying BMT content, and it generally shows a comparably small hysteresis with a nearly linear increase with the electric field. Similar to the remnant polarization and piezoelectric property, the unipolar strain first increases significantly with the increase in the BMT content and then reaches the maxima of 0.174% at  $x = 0.08$ , finally starts to decrease. It is probably due to the easy polarization switching around the MPB composition by the coexistence of rhombohedral and tetragonal phases.<sup>32</sup> In addition, the normalized strain  $d_{33}^*$  shows the same trend (see inset of Fig. 8), and the highest  $d_{33}^*$  of 436 pm/V was obtained at the MPB composition of  $x = 0.08$ , which shows a great potential for the design of piezoelectric actuators. For a better understanding of the strain behavior of the  $x = 0.08$  sample, the frequency dependence of the strain

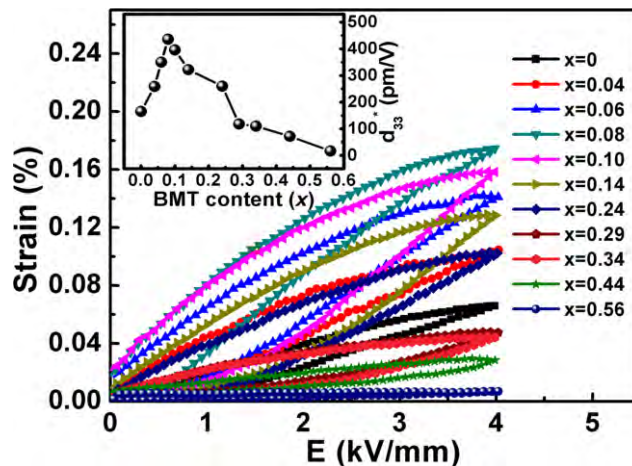


Fig. 8. Unipolar strain curves at 1 Hz for  $x$ BMT–PZ–PT ceramics with different BMT contents and the inset shows the normalized strain  $d_{33}^*$  as a function of the BMT content.

values and the corresponding  $d_{33}^*$  were also measured. The results indicate that the  $x = 0.08$  sample exhibited a frequency-insensitive strain behavior. Its value ranges only between 0.168% and 0.178% as frequency increases from 0.5 to 40 Hz and the normalized strain  $d_{33}^*$  varies between 419 and 445 pm/V.

#### IV. Conclusions

A new piezoelectric composition system of  $x$ BMT–(0.56 –  $x$ ) PZ–0.44PT ( $x$ BMT–PZ–PT) was constructed by substituting BMT for PZ and fabricated by a conventional mixed-oxide method. The phase transitional behaviors and composition-dependent electrical properties were investigated as a function of the BMT content. The XRD results indicate that the ternary system undergoes a gradual phase structural transformation with changing the BMT content. Consequently, an MPB was identified at  $x = 0.08$ , which was also confirmed by corresponding dielectric, piezoelectric, and ferroelectric properties. With increasing the BMT content, the dielectric diffuseness and frequency dispersion behavior were induced and the solid solutions were found to exhibit a normal-relax-or-diffuse ferroelectric transformation from the PZ-rich side to the BMT-rich side. The  $x = 0.08$  composition possessed the optimum properties of  $\epsilon_{33}^T/\epsilon_0 = 1450$ ,  $Q_m = 69$ ,  $d_{33} = 390$  pC/N,  $k_p = 0.46$ ,  $P_r = 30$   $\mu\text{C}/\text{cm}^2$ ,  $E_c = 1.4$  kV/mm and  $T_c = 325^\circ\text{C}$ , and a strain with 0.174% ( $d_{33}^* = 436$  pm/V) under an electric field of 4 kV/mm was obtained. Furthermore, the  $x = 0.08$  sample exhibited a good thermal-depolarization behavior with a  $d_{33}$  value of  $>315$  pC/N up to  $290^\circ\text{C}$ , and a frequency-insensitive strain behavior. These results demonstrate that this ternary system could be a good piezoelectric material with reduced lead content and interesting electrical properties.

#### Acknowledgments

Financial support from the National Natural Science Foundation of China (Grant nos. 51272060 and 51332002), and an opening fund of State Key Laboratory of New Ceramic and Fine Processing at Tsinghua University is gratefully acknowledged.

#### References

1. B. Jaffe, W. R. Cook, and H. Jaffe, *Piezoelectric Ceramics*. Academic Press, New York, NY, 1971.
2. G. H. Haertling, "Ferroelectric Ceramics: History and Technology," *J. Am. Ceram. Soc.*, **82** [4] 797–818 (1999).
3. R. Guo, L. E. Cross, S. E. Park, B. Noheda, D. E. Cox, and G. Shirane, "Origin of the High Piezoelectric Response in  $\text{PbZr}_{1-x}\text{Ti}_x\text{O}_3$ ," *Phys. Rev. Lett.*, **84** [23] 5423–6 (2000).

- <sup>4</sup>H. X. Fu and R. E. Cohen, "Polarization Rotation Mechanism for Ultra-High Electromechanical Response in Single-Crystal Piezoelectrics," *Nature*, **403**, 281–3 (2000).
- <sup>5</sup>W. W. Cao and L. E. Cross, "Theoretical Model for the Morphotropic Phase Boundary in Lead Zirconate-Lead Titanate Solid Solution," *Phys. Rev. B*, **47**, 4825–30 (1993).
- <sup>6</sup>V. Koval, C. Alemany, J. Briancin, H. Brunckova, and K. Saksl, "Effect of PMN Modification on Structure and Electrical Response of  $x$ PMN– $(1-x)$ PZT Ceramic Systems," *J. Eur. Ceram. Soc.*, **23**, 1157–66 (2003).
- <sup>7</sup>M. Kobune, K. Muto, and Y. Akiyama, "Piezoelectric and Ferroelectric Properties of  $\text{Pb}(\text{Zn}_{1/3}\text{Nb}_{2/3})\text{O}_3$ – $\text{PbTiO}_3$ – $\text{PbZrO}_3$  Ceramics," *Jpn. J. Appl. Phys.*, **110** [1] 12–7 (2002).
- <sup>8</sup>N. Vittayakorn, G. Rujijjanagul, X. L. Tan, M. A. Marquardt, and D. P. Cann, "The Morphotropic Phase Boundary and Dielectric Properties of the  $x\text{Pb}(\text{Zr}_{1/2}\text{Ti}_{1/2})\text{O}_3$ – $(1-x)\text{Pb}(\text{Ni}_{1/3}\text{Nb}_{2/3})\text{O}_3$  Perovskite Solid Solution," *J. Appl. Phys.*, **96** [9] 5103–9 (2004).
- <sup>9</sup>T. R. Shrout and S. J. Zhang, "Lead-Free Piezoelectric Ceramics: Alternatives for PZT?" *J. Electroceram.*, **19** [1] 111–24 (2007).
- <sup>10</sup>M. E. Line and A. M. Glass, *Principles and Applications of Ferroelectric and Related Materials*. Oxford University Press, London, 1977.
- <sup>11</sup>M. M. Kumar, V. R. Palkar, K. Srinivas, and S. V. Suryanarayana, "Ferroelectricity in a Pure  $\text{BiFeO}_3$  Ceramic," *Appl. Phys. Lett.*, **76** [19] 2764–6 (2000).
- <sup>12</sup>A. A. Belik, S. Iikubo, K. Kodama, N. Igawa, S. Shamoto, M. Maie, T. Nagai, Y. Matsui, S. Y. Stefanovich, B. I. Lazoryak, and E. T. Muromachi, " $\text{BiScO}_3$ : Centrosymmetric  $\text{BiMnO}_3$ -Type Oxide," *J. Am. Chem. Soc.*, **128** [3] 706–7 (2005).
- <sup>13</sup>Y. Inaguma and T. Katsumata, "High Pressure Synthesis, Lattice Distortion, and Dielectric Properties of a Perovskite  $\text{Bi}(\text{Ni}_{1/2}\text{Ti}_{1/2})\text{O}_3$ ," *Ferroelectrics*, **286**, 111–7 (2003).
- <sup>14</sup>D. D. Khalyavin, A. N. Salak, N. P. Vyshatko, A. B. Lopes, N. M. Olekhnovich, A. V. Pushkarev, I. I. Maroz, and Y. V. Radyush, "Crystal Structure of Metastable Perovskite  $\text{Bi}(\text{Mg}_{1/2}\text{Ti}_{1/2})\text{O}_3$ : Bi-Based Structural Analogue of Antiferroelectric  $\text{PbZrO}_3$ ," *Chem. Mater.*, **18** [21] 5104–10 (2006).
- <sup>15</sup>T. T. Qi, I. Grinberg, and A. M. Rappe, "First-Principles Investigation of the Highly Tetragonal Ferroelectric Material  $\text{Bi}(\text{Zn}_{1/2}\text{Ti}_{1/2})\text{O}_3$ ," *Phys. Rev. B*, **79** [9] 094114, 5pp (2009).
- <sup>16</sup>Y. Yoneda, H. Saitoh, K. Yoshii, T. Nishida, H. Hayakawa, and N. Ikeda, "Growth and Characterization of Bismuth Magnesium Titanate  $\text{Bi}(\text{Mg}_{1/2}\text{Ti}_{1/2})\text{O}_3$ ," *Key Eng. Mater.*, **421–422**, 30–3 (2010).
- <sup>17</sup>C. A. Randall, R. Eitel, B. Jones, and T. R. Shrout, "Investigation of a High  $T_c$  Piezoelectric System:  $(1-x)\text{Bi}(\text{Mg}_{1/2}\text{Ti}_{1/2})\text{O}_3$ – $x\text{PbTiO}_3$ ," *J. Appl. Phys.*, **95**, 3633–8 (2004).
- <sup>18</sup>M. D. Snel, W. A. Groen, and G. D. With, "Investigation of the New Piezoelectric System  $(1-x)\text{Bi}(\text{MgTi})_{0.5}\text{O}_3$ – $x\text{PbTiO}_3$ ," *J. Eur. Ceram. Soc.*, **25**, 3229–33 (2005).
- <sup>19</sup>J. Chen, X. L. Tan, W. Jo, and J. Rödel, "Temperature Dependence of Piezoelectric Properties of High- $T_c$   $(1-x)\text{Bi}(\text{Mg}_{1/2}\text{Ti}_{1/2})\text{O}_3$ – $x\text{PbTiO}_3$ ," *J. Appl. Phys.*, **106**, 034109, 8pp (2009).
- <sup>20</sup>Q. Zhang, Z. R. Li, F. Li, Z. Xu, and X. Yao, "Temperature Dependence of Dielectric/Piezoelectric Properties of  $(1-x)\text{Bi}(\text{Mg}_{1/2}\text{Ti}_{1/2})\text{O}_3$ – $x\text{PbTiO}_3$  Ceramics with an MPB Composition," *J. Am. Ceram. Soc.*, **93** [10] 3330–4 (2010).
- <sup>21</sup>J. Chen, J. Y. Li, L. L. Fan, N. Zou, P. F. Ji, and L. Liu, "Enhanced Piezoelectric and Antiferroelectric Properties of High- $T_c$  Perovskite of Zr-substituted  $\text{Bi}(\text{Mg}_{1/2}\text{Ti}_{1/2})\text{O}_3$ – $\text{PbTiO}_3$ ," *J. Appl. Phys.*, **112** [07] 4101–6 (2012).
- <sup>22</sup>J. Fu and R. Z. Zuo, "Giant Electrostrains Accompanying the Evolution of a Relaxor Behavior in  $\text{Bi}(\text{Mg}_{0.5}\text{Ti}_{0.5})\text{O}_3$ – $\text{PbZrO}_3$ – $\text{PbTiO}_3$  Ferroelectric Ceramics," *Acta Mater.*, **61**, 3687–91 (2013).
- <sup>23</sup>K. Uchino and S. Nomura, "Critical Exponents of the Dielectric Constants in Diffused-Phase-Transition Crystals," *Ferroelectrics*, **44**, 55–61 (1982).
- <sup>24</sup>Z. G. Zhu, K. Jiang, G. J. Davies, G. R. Li, Q. R. Yin, and S. Z. Sheng, "Dielectric Relaxation Behavior in  $\text{Pb}(\text{Mn}_{1/3}\text{Sb}_{2/3})\text{O}_3$ – $\text{Pb}(\text{Zr}, \text{Ti})\text{O}_3$  Systems," *Smart Mater. Struct.*, **15**, 1249–54 (2006).
- <sup>25</sup>W. Chen, X. Yao, and X. Y. Wei, "Tunability and Ferroelectric Relaxor Properties of Bisbuth Strontium Titanate Ceramics," *J. Appl. Phys.*, **90** [18] 182902, 3pp (2007).
- <sup>26</sup>V. V. Shvartsman, W. Kleemann, J. Dec, Z. K. Xu, and S. G. Lu, "Diffuse Phase Transition in  $\text{BaTi}_{1-x}\text{Sn}_x\text{O}_3$  Ceramics: An Intermediate State between Ferroelectric and Relaxor Behavior," *J. Appl. Phys.*, **99**, 124111, 8pp (2006).
- <sup>27</sup>V. Porokhonsky, S. Kamba, A. Pashkin, M. Savinov, R. E. Eitel, and C. A. Randall, "Broadband Dielectric Spectroscopy of  $(1-x)\text{BiScO}_3$ – $x\text{PbTiO}_3$  Piezoelectrics," *Appl. Phys. Lett.*, **83** [8] 1605–7 (2003).
- <sup>28</sup>R. Z. Zuo, Y. Liu, S. Su, X. C. Chu, and X. H. Wang, "Phase Transformation Behavior and Electrical Properties of  $\text{Pb}(\text{Zr}_{0.56}\text{Ti}_{0.44})\text{O}_3$ – $\text{Bi}(\text{Zn}_{0.5}\text{Ti}_{0.5})\text{O}_3$  Solid Solution Ceramics," *J. Am. Ceram. Soc.*, **94** [12] 4340–4 (2011).
- <sup>29</sup>R. Z. Zuo, J. Fu, S. B. Lu, and Z. K. Xu, "Normal to Relaxor Ferroelectric Transition and Domain Morphology Evolution in  $(\text{K},\text{Na})(\text{Nb},\text{Sb})\text{O}_3$ – $\text{LiTaO}_3$ – $\text{BaZrO}_3$  Lead-Free Ceramics," *J. Am. Ceram. Soc.*, **94** [12] 4352–7 (2011).
- <sup>30</sup>J. Ricote, R. W. Whatmore, and D. J. Barber, "Studies of the ferroelectric domain configuration and polarization of rhombohedral PZT ceramics," *J. Phys.: Condens. Matter*, **12**, 323–37 (2000).
- <sup>31</sup>D. A. Berlincourt, C. Cmolik, and H. Jaffe, "Piezoelectric Properties of Polycrystalline Lead Titanate Zirconate Compositions," *Proc. IRE*, **48** [2] 220–9 (1960).
- <sup>32</sup>C. A. Randall, N. Kim, J. P. Kucera, W. W. Cao, and T. R. Shrout, "Intrinsic and Extrinsic Size Effects in Fine-Grained Morphotropic-Phase-Boundary Lead Zirconate Titanate Ceramics," *J. Am. Ceram. Soc.*, **81** [3] 677–88 (1998).
- <sup>33</sup>T. T. Wang and J. Yu, "Piezoelectric Properties of  $\text{Pb}_{0.85}\text{Bi}_{0.15}(\text{Zr}_{0.442}\text{Ti}_{0.483}\text{Zn}_{0.075})\text{O}_3$  Ceramics," *Ferroelectrics*, **408**, 20–4 (2010).
- <sup>34</sup>T. Sareein, W. Hu, X. Tan, and R. Yimnirun, "The Morphotropic Phase Boundary in the  $(1-x)\text{PbZrO}_3$ – $x[0.3\text{Bi}(\text{Zn}_{1/2}\text{Ti}_{1/2})\text{O}_3$ – $0.7\text{PbTiO}_3]$  Perovskite Solid Solution," *J. Mater. Sci.*, **47**, 1774–9 (2012).
- <sup>35</sup>A. Dwivedi and C. A. Randall, "Morphotropic Phase Boundary in High Temperature Ferroelectric  $x\text{Bi}(\text{Zn}_{1/2}\text{Ti}_{1/2})$ – $y\text{PbZrO}_3$ – $z\text{PbTiO}_3$  Perovskite Ternary Solution," *Mater. Lett.*, **65**, 1308–11 (2011).
- <sup>36</sup>H. J. Kang, J. Chen, L. J. Liu, C. Z. Hu, L. Fang, and X. R. Xing, "Structure and Enhanced Piezoelectric Response by Chemical Doping in  $\text{PbTiO}_3$ – $\text{PbZrO}_3$ – $\text{Bi}(\text{Ni}_{1/2}\text{Ti}_{1/2})\text{O}_3$ ," *Inorg. Chem. Commun.*, **31**, 66–8 (2013).
- <sup>37</sup>W. Hu, X. L. Tan, and K. Rajan, "Piezoelectric Ceramics with Compositions at the Morphotropic Phase Boundary in the  $\text{BiFeO}_3$ – $\text{PbZrO}_3$ – $\text{PbTiO}_3$  Ternary System," *J. Am. Ceram. Soc.*, **94** [12] 4358–63 (2011). □